

Supplementary Materials

Materials & Methods

Chemicals used and SAM preparation

All chemicals used (Table 1) were purchased from Sigma-Aldrich (St. Louis, MO) and used as received unless stated otherwise. Thiol solutions for SAM formation and grafting were prepared in >99.5% 2-butanol. The SAMs were prepared on an ultraflat patch of template-stripped gold, which was prepared according to the procedure described by Hegner et al.¹ In short, the procedure can be summarized in three steps: (i) First, a 0.25 cm² piece of mica coated with a 300 nm thick layer of gold (Georg Albert PVD-Beschichtungen, Heidelberg, Germany) was glued to a clean glass slide, with its gold side pointing downward, using a two-component epoxy glue (type 377, Epoxy Technology Inc., Waterloo, Belgium), leaving the mica side exposed to air. (ii) Subsequently, the sample was heated at 150 °C for 2 h, which activates the hardening process of the glue. (iii) Finally, the sample was submerged in a solution of tetrahydrofuran (THF) for 5 min, after which it can be stripped at the gold–mica interface, removing the mica. After stripping, the sample was immediately submerged in a freshly prepared solution of 5 mM of alkanethiol in 2-butanol. After incubation for >18 h in the thiol solution, the gold sample was washed with ethanol (99.8%) and dried with a gentle flow of nitrogen.

Atomic Force Microscopy

Imaging and nanografting were performed using a MultiMode AFM with a Nanoscope IV controller (Veeco, Santa Barbara, CA, USA) equipped with an E-type piezo scanner (XY-range ~12 μm) and a liquid-cell (MTFML, Veeco) holding the cantilever. The AFM system was calibrated by using a 1 x 1 μm² (100 nm-deep) calibration grid. After calibration the sample was placed in the liquid-cell and subsequently submerged in a 50 μl droplet of a 5 mM 2-butanol solution of an alkanethiol. The whole sample and droplet were then enclosed by a fluorosilicate O-ring (FSFCO-10, Veeco). A laser beam was focused on the end point of a V-shaped Si₃N₄ NP-S cantilever (Veeco; cantilever A on the NP-S chip, nominal spring constant 0.58 N/m), which had been cleaned by rinsing with chloroform and by irradiation with UV light (20 min.). Moreover, directly prior to every experiment the cantilever was rinsed with ethanol (99.8%). The laser beam was deflected onto a four-quadrant photosensitive detector, the monitored vertical deflection was interpreted as the topography while the horizontal deflection, caused by the torsional deformation of the cantilever when its tip scans over the surface, was interpreted as the lateral friction force between tip and sample.

Imaging was performed in contact mode, under a low load force of $F_N \approx 6$ nN (~1V deflection set point) at 1 Hz (~4 μm s⁻¹ for a 2 x 2 μm² image), these conditions were chosen to avoid compression and deformation of the monolayers.² The pressure that the tip then exerts is ~0.5 GPa, as calculated by the Hertzian model³ assuming a tip radius of 15 nm and a contact area of 12 nm². Nanoshaving of the SAM was performed at a high load force of $F_N \approx 120$ nN (~20 V) at 15 Hz (~60 μm s⁻¹), and the exerted pressure is ~ 10 GPa.

Data and images were analyzed by using NanoScope 6.13 and Origin 8 software. The friction was determined from both trace and retrace of the lateral force images, these data were analyzed off-line by subtracting both channels (raw data) and divided by 2 for averaging, and subsequently converted into friction data (nN) using the method outlined below. For statistics, the height data were analyzed by taking consecutive cross sections (sampling over 20-50 lines) via step size determination on the edges of the nanografted patch on a single gold terrace within the software. Per image, $N \geq 5$ of these samplings were performed. Subsequently, at least three images per nanografted patch were analyzed per experiment (up and down scans), and also at least three independent experiments in total (all with different cantilevers, to exclude the possibility that differences in friction are caused by differences in tip shape). The friction was determined only in the $450 \times 450 \text{ nm}^2$ center region of the $500 \times 500 \text{ nm}^2$ nanografted patches to eliminate edge effects. Furthermore, the friction was collected for the same amount and set of images as the topography analysis with a sampling of three on every image. In addition to the friction measurements of the nanografted patches in all experiments, the friction of the SAM matrix was determined in order to ascertain the quality and reliability of the measurements and, when necessary, to exclude measurements from further analysis. For all analyzed data, errors given are $\pm \text{S.D.}$.

Quantifying the AFM data

V-shaped NP-S cantilevers (Veeco) were calibrated combining the Sader method⁴ and the thermal oscillation method,⁵ with some minor practical adaptations. In short, the vertical, torsional, and lateral spring constants of the V-shaped cantilever were determined by the following method. The vertical spring constant was determined by using the thermal tune software module of the NS V system (Veeco) by fitting the primary resonance peak with the simple harmonic oscillator model.⁶ The system can process the data for resonances up to 100 kHz.⁷ After a deflection sensitivity (from now designated as InvOLS; inverse optical lever sensitivity) calibration in air of the cantilever mounted in the setup ($N=5$), we used the Hutter and Bechhoefer method⁵ - with the later described corrections for a V-shaped cantilever,^{7,8} to determine the vertical spring constant. The torsional and physically related lateral spring constant for a V-shaped cantilever was calculated by using the parallel beam approach for a composite ceramic-gold cantilever.⁹⁻¹² The following formulas were used to calculate the lateral spring constant,

$$k_{lat} = \frac{4}{3 \cos^2 \theta + 6 \cdot (1 + \nu) \cdot \sin^2 \theta} \left(\frac{L}{H} \right)^2 \times k_z,$$

and the torsional spring constant,

$$k_{tors} = k_{lat} H^2$$

where θ is the inner angle between the cantilever beam and the substrate, ν is the Poisson ratio, L is the length of the cantilever, H is the height of the tip, and k_z is the vertical spring constant. For the NP-S cantilever (cantilever A of the chip) the (nominal) dimensions given by the manufacturer are $\theta = 62^\circ$, $\nu = 0.24$ (for Si_3N_4),¹³ $L = 115 \mu\text{m}$, $w = 25 \mu\text{m}$ (width), $H = 3 \mu\text{m}$, $\Delta L = 4 \mu\text{m}$ (tip set-back), $t = 0.6 \mu\text{m}$ (thickness), and $R = 10-20 \text{ nm}$ (tip radius). We determined an overall vertical spring constant of $k_z = 252 \pm 19 \text{ pN/nm}$ ($\pm \text{S.D.}; N = 6$; all chips from one wafer) by the method described above (note the 57% difference with the manufacturer's data). By using the formulas above, we calculated a lateral spring constant of $k_{lat} = 159 \pm 20 \text{ N/m}$ and a torsional spring

constant of $k_{tors} = (2.06 \pm 0.15) \times 10^{-9}$ Nm/rad. We determined a vertical InvOLS for the setup in 2-butanol (note: different from that in air¹⁴) of 23.76 ± 0.43 nm/V (\pm S.D.) and a horizontal InvOLS of 0.77 ± 0.10 nm/V (\pm S.D.), which leads to an overall conversion rate for the photodetector data (in volt) to the contact force (in newton) of 5.98 ± 0.46 nN/V and for the friction force of 0.123 ± 0.017 nN/mV.

Molecular model

The apparent height of the molecules in the SAM was calculated using data from literature;¹⁵ bond lengths are 1.523 Å (C-C), 2.293 Å (S-Au), 1.815 Å (C-S), 1.338 Å (C-O), 1.208 Å (C=O), 1.438 Å (C-N) and the angle between the Au-S-C and C-C-C bonds in the alkyl backbone is in both cases 109.5°. The hydrogen bond between COOH-dimers is 3.72 Å (C-C distance) and 3.07 Å (N-N distance), as was found in literature and verified with DFT:B3LYP/3-21G calculations using the GAMESS¹⁶ interface of ChemBio3D Ultra 11.0. With these data, the expected lengths of the alkanethiols were calculated using ChemBio3D Ultra 11.0. Subsequently, by taking into account a 30° tilt (if not stated otherwise) for the molecules,^{17,18} the apparent height or thickness of the layer was calculated.

Supplementary references

1. M. Hegner, P. Wagner and G. Semenza, *Surf. Sci.*, 1993, **291**, 39.
2. M. Castronovo, F. Bano, S. Raugei, D. Scaini, M. Dell'Angela, R. Hudej, L. Casalis and G. Scoles, *J. Am. Chem. Soc.*, 2007, **129**, 2636.
3. E. Barrena, C. Ocal and M. Salmeron, *J. Chem. Phys.*, 2000, **113**, 2413.
4. J. E. Sader, I. Larson, P. Mulvaney and L. R. White, *Rev. Sci. Instrum.*, 1995, **66**, 3789.
5. J. L. Hutter and J. Bechhoefer, *Rev. Sci. Instrum.*, 1993, **64**, 1868.
6. J. E. Sader, J. W. M. Chon and P. Mulvaney, *Rev. Sci. Instrum.*, 1999, **70**, 3967.
7. B. Ohler, *Rev. Sci. Instrum.*, 2007, **78**, 0637011.
8. R. W. Stark, T. Drobek and W. M. Heckl, *Ultramicroscopy*, 2001, **86**, 207.
9. A. Noy, C. D. Frisbie, L. F. Rozsnyai, M. S. Wrighton and C. M. Lieber, *J. Am. Chem. Soc.*, 1995, **117**, 7943.
10. J. E. Sader, *Rev. Sci. Instrum.*, 1995, **66**, 4583.
11. J. E. Sader and R. C. Sader, *Appl. Phys. Lett.*, 2003, **83**, 3195.
12. J. L. Hazel and V. V. Tsukruk, *Thin Solid Films*, 1999, **339**, 249.
13. W. Alexander and J. F. Shackelford, *CRC Materials Science and Engineering Handbook* (p.537), CRC Press/Taylor and Francis, Boca Raton, 2001.
14. E. Tocha, J. Song, H. Schönherr and G. J. Vancso, *Langmuir*, 2007, **23**, 7078.
15. D. R. Lide, *Handbook of Chemistry and Physics. 89th Edition*, CRC Press/Taylor and Francis, Boca Raton, 2008-2009.
16. M. W. Schmidt, K. K. Baldridge, J. A. Boatz, S. T. Elbert, M. S. Gordon, J. H. Jensen, S. Koseki, N. Matsunaga, K. A. Nguyen, S. J. Su, T. L. Windus, M. Dupuis and J. A. Montgomery, *J. Comput. Chem.*, 1993, **14**, 1347.
17. M. D. Porter, T. B. Bright, D. L. Allara and C. E. D. Chidsey, *J. Am. Chem. Soc.*, 1987, **109**, 3559.
18. J. C. Love, L. A. Estroff, J. K. Kriebel, R. G. Nuzzo and G. M. Whitesides, *Chem. Rev.*, 2005, **105**, 1103.

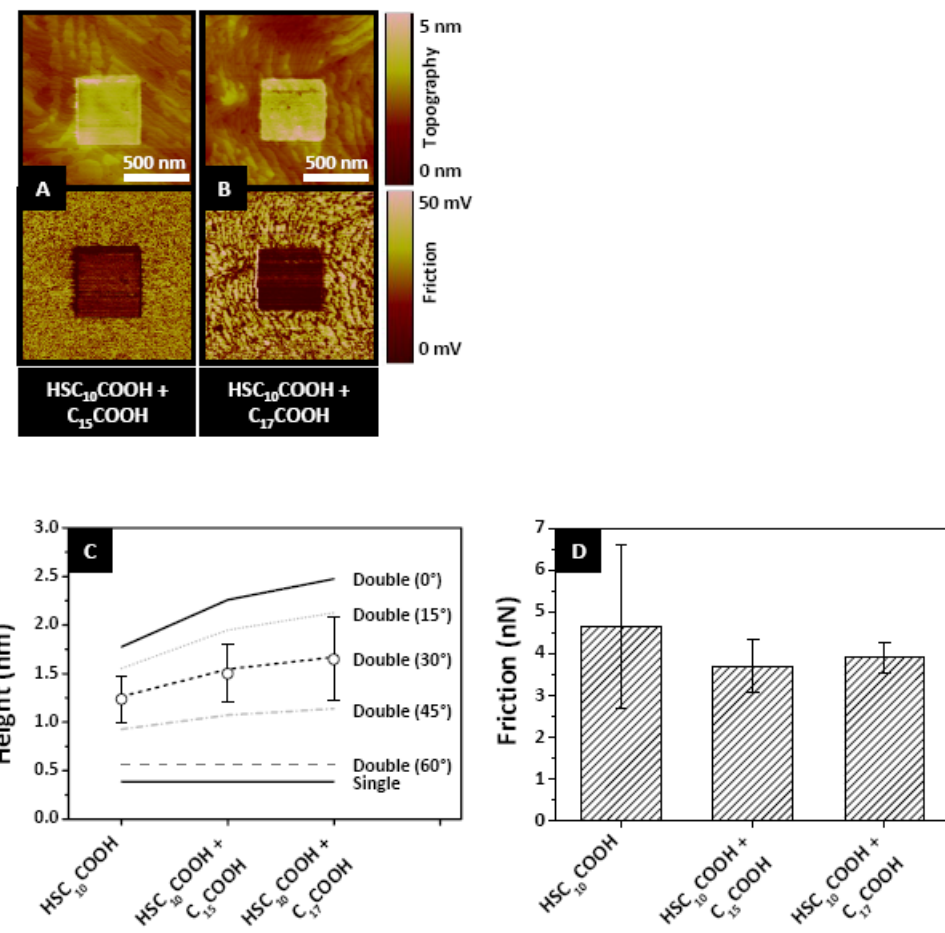


Figure S1. AFM topography (top row) and friction images (retrace, bottom row) of HSC₁₀COOH nanografted patches grafted in the presence of 9 equivalents (A) 1-hexadecanoic acid C₁₅COOH, and (B) 1-octadecanoic acid C₁₇COOH. (C) Heights of the nanografted patches compared to a pure HSC₁₀COOH-HOOCC₁₀SH nanograft and the expected heights according to a single layer or a double layer model with interlayer angles of 0°, 15°, 30°, 45° and 60°. (D) Lateral friction values of the nanografts. All data are \pm S.D. ($N \geq 10$).

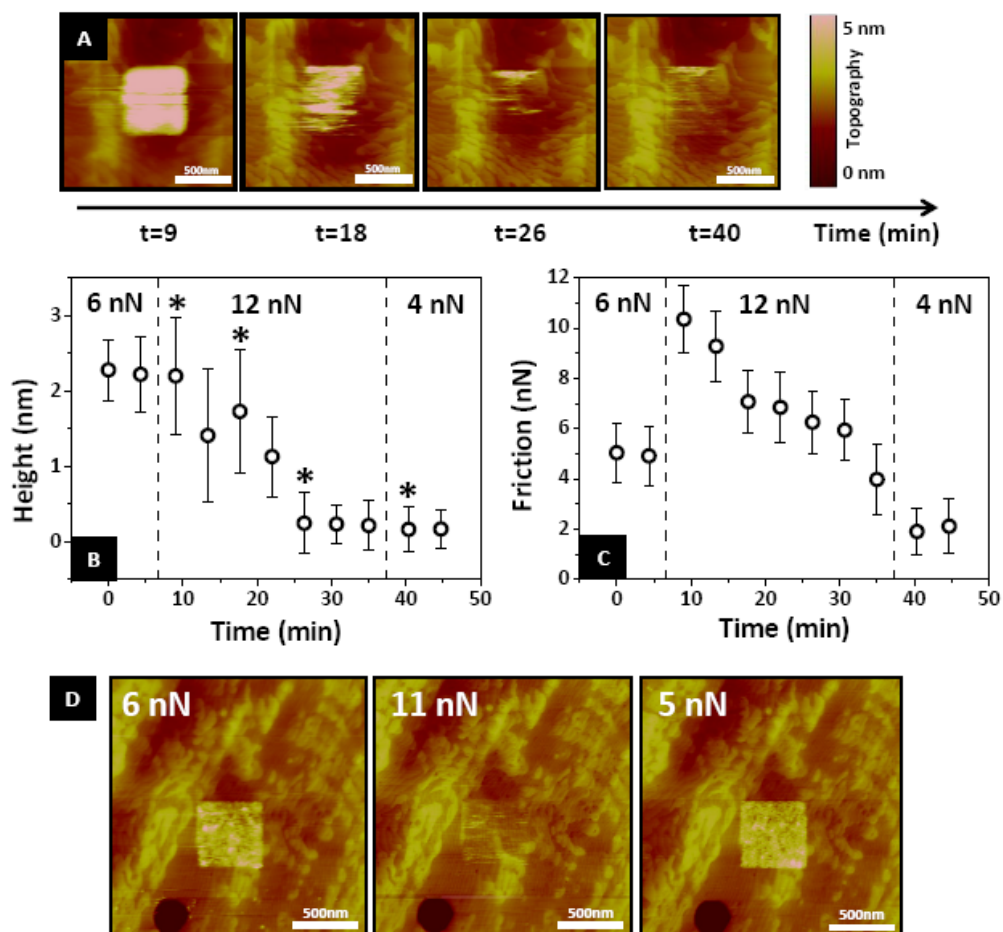


Figure S2. Mechanical stability test of an $\text{HSC}_{11}\text{NH}_2$ nanografted patch in a HSC_8 matrix performed by varying the load performed with the AFM tip. The tip scan speed is kept constant at $8 \mu\text{m}/\text{s}$. (A) Series of topography and friction images following an $\text{HSC}_{11}\text{NH}_2$ nanografted patch in a 2-butanol supernatant solution over time. (B) Height variation of the nanografted patch over time. The nanografted patch was created and imaged at $t=0$ at a 6 nN load, thereafter the load was increased to 12 nN. At $t=37$ the load was decreased to 3 nN, but the nanograft did not reform. (C) Corresponding friction of the nanografted patch over time. (D) Series of AFM topography images of an $\text{HSC}_{11}\text{NH}_2$ nanografted patch imaged at successively 6 nN, 11 nN and 5 nN, showing the removal and reformation of the nanograft.

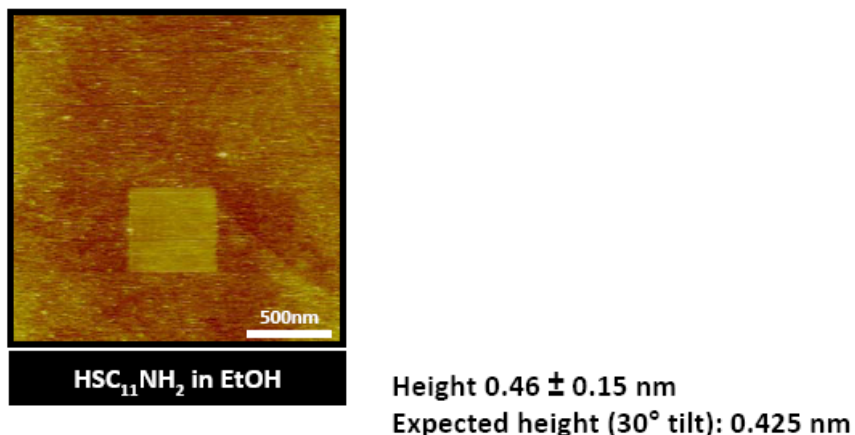


Figure S3. AFM topography image of a HSC₁₁NH₂ patch nanografted in a HSC₈ matrix SAM from an ethanolic solution. The observed relative height of the graft is 0.46 ± 0.15 nN, which corresponds to a monolayer of HSC₁₁NH₂ (expected height 0.425 nm at a 30° tilt). All data are ± S.D. ($N \geq 10$).